AJNR

The wedge-shaped cord terminus: a radiographic sign of caudal regression.

A J Barkovich, N Raghavan, S Chuang and W W Peck

AJNR Am J Neuroradiol 1989, 10 (6) 1223-1231
http://www.ajnr.org/content/10/6/1223

The Wedge-Shaped Cord Terminus: A Radiographic Sign of Caudal Regression

A. James Barkovich[1,2]
Narasimhachari Raghavan[1]
Sylvester Chuang[3]
Wallace W. Peck[4]

Imaging studies from 13 patients with caudal regression were reviewed retrospectively to assess the spectrum and findings of this anomaly. Seven patients were evaluated with MR and six with myelography (supplemented with CT in three). The level of regression varied from T9 to the coccyx. Although osseous abnormalities were more readily identified and characterized by CT, MR effectively depicted the level of vertebral regression, presence of central spinal stenosis, and vertebral dysraphic anomalies. MR demonstrated a characteristic wedge-shaped (longer dorsally) cord terminus in seven of the patients. When this characteristic cord terminus is seen, imaging of the lower lumbar and sacral regions should be performed to verify the diagnosis of caudal regression. Tethered spinal cords have been described in patients with caudal regression and were seen in two of our patients.

We present the first cases of individuals who have survived with absence of vertebrae above the T10 level and an unusual case of caudal regression with absent lumbar vertebrae and preserved lower sacral and coccygeal vertebrae. The syndrome of caudal regression encompasses a wide spectrum of pathology that is analyzed well by modern imaging techniques.

***AJNR* 10:1223–1231, November/December 1989**

The spectrum of caudal regression syndrome ranges from isolated asymptomatic coccygeal aplasia to absent sacral, lumbar, and thoracic vertebrae with associated severe neurologic deficits [1, 2]. Most patients are initially evaluated for orthopedic and urologic complaints, but some present with progressive neurologic deficits resulting from tethering of the spinal cord that may be amenable to surgical therapy. Tethering may result from dural sac stenosis or from a lesion that prevents ascent of the spinal cord during growth [2]. Traditionally, positive contrast myelography supplemented by CT has been the study of choice. Recently, MR has been shown to be of great value in the imaging of congenital spine anomalies [3]. Moreover, the noninvasive nature of MR makes it especially advantageous in young, debilitated patients such as many of those with caudal regression. In this article, the MR, myelographic, and CT-myelographic appearance of 13 patients with caudal regression is evaluated and related to the pathologic features and embryogenesis of the syndrome.

Subjects and Methods

Imaging studies were retrospectively evaluated in 13 patients with caudal regression syndrome. Seven patients were studied by MR (Table 1) and six by myelography (supplemented with CT in three) (Table 2). The average age of the four girls and nine boys was 8 years old (range, 3 weeks to 19 years). They initially presented with neurogenic bladder (eight), anal atresia (three), renal dysplasia (one), orthopedic deformities (three), and extrophy of the bladder (one). (Several patients had more than one presenting symptom.)

Received March 14, 1989; revision requested May 18, 1989; revision received June 5, 1989; accepted June 7, 1989.

The views expressed in this article are those of the authors and do not reflect the official policy or position of the Department of the Army, Department of Defense, or the U.S. Government.

[1] Department of Radiology, Section of Neuroradiology, L-371; University of California School of Medicine, San Francisco, CA 94143. Address reprint requests to Medical Editing HSHH-CI-ME, Department of Clinical Investigation, Letterman Army Medical Center, Presidio of San Francisco, CA 94129-6700.

[2] Department of Radiology, Letterman Army Medical Center, Presidio of San Francisco, CA 94129-6700.

[3] Department of Radiology, The Hospital for Sick Children, Toronto, Ontario M5G 1X8, Canada.

[4] Department of Radiology, St Joseph's Hospital, Orange, CA 92668.

0195-6108/89/1006-1223

Five patients were studied on a GE 1.5-T whole-body superconductive magnet with surface receiving coils, and two were examined on a 0.35-T Diasonics magnet. Technique included spin-echo (SE) sequences with data obtained in either 128 or 256 views in the phase-encoding direction and 256 views in the readout direction with a two-dimensional Fourier transform reconstruction algorithm. The field of view ranged from 20 to 30 cm depending on imaging plane. All patients were imaged in a supine position in the scanner with sagittal 3- to 5-mm-thick sections and 500–1000/20–70/2–4 (TR/TE/excitations). Five-millimeter-thick axial SE sections with 650–1000/20–40 were available in five of seven patients.

Six patients had myelograms that in three were supplemented with CT. Myelograms were performed after intrathecal administration of 3 to 5 ml of metrizamide (170 mg I/ml) installed via cervical or lumbar

TABLE 1: Summary of Patient Data for Caudal Regression as Determined by MR

Patient No.	Age at Imaging	Clinical Presentation	Vertebrae		Level of Cord Terminus	Shape of Cord Terminus	Myelomalacia/ Syringohydromyelia	Tethering Lesion	Bony Spinal Canal Stenosis	Bony Abnormality
			Last Intact	Last						
1	7 yr	Neurogenic bladder; clubfoot	L3	L4	Mid-T10	Blunted/oblique	No	No	Severe at L3	Fused L3, L4
2	16 yr	Anal atresia; hydrocephalus caused by aqueductal stenosis	S1	S2	L3–L4	Tapered, stretched	Yes	Fibrolipoma of filum	No	L4–L5 congenital fusion; spina bifida of L1
3	15 yr	Neurogenic bladder	S1	S2	Mid-T11	Blunted/oblique, longer dorsally	No	No	Stenotic from L2 inferiorly	Hypoplastic spinous process of L5
4	14 yr	Neurogenic bladder	S1	S2	T11–T12	Blunted/oblique, longer dorsally	No	No	Marked from L4 inferiorly	Absent L5 spinous process
5	8 mo	Urinary bladder extrophy	T7	T8	T5	Blunted/oblique, longer dorsally	NA	No	Severe at T7–T8	Absent T8 spinous process
6	14 yr	Neurogenic bladder	S1	S2	T12–L1	Blunted/oblique, longer dorsally	No	No	No	Spina bifida of S2
7	7 yr	Neurogenic bladder; lower extremity weakness	S1	S3	T12–L1	Blunted/oblique, longer dorsally	No	No	No	Spina bifida of S2

TABLE 2: Summary of Patient Data for Caudal Regression as Determined by CT-Myelography

Patient No.	Age at Imaging	Clinical Presentation	Vertebrae		Level of Cord Terminus	Shape of Cord Terminus	Myelomalacia/ Syringohydromyelia	Tethering Lesion	Bony Spinal Canal Stenosis	Bony Abnormality
			Last Intact	Last						
8	1 mo	Anal atresia	S1	NA	S3–S4	Bulbous	NA	Lipomatous	No	Dysraphic S2
9	3 wk	Bilateral renal dysplasia	L1	L2	T9–T10	Blunted/oblique, longer dorsally	NA	NA	NA	Fused L1, L2 articulate with ilia
10	3 yr	Neurogenic bladder	T9	T9	T8–T9	Oblique, not well seen	NA	No	No	T9 spina bifida; ilia articulate with sacrum
11	2 yr	Bilateral hip dislocations; anal atresia	T8	T9	Mid-thoracic spine	NA	NA	No	NA	Absent lower thoracic and entire lumbar spine; sacrum present with spina bifida
12	19 yr	Neurogenic bladder	S1	S2	Mid-T12	Bulbous (no lat)	NA	NA	Yes S1, S2	Duplex spinous process of S1
13	4 yr	Club foot; neurogenic bladder	L5	S1	NA	NA	NA	NA	NA	Ilia articulate with L5

puncture. Anteroposterior and lateral radiographs were obtained in five cases and only anteroposterior myelographic films were available in a single patient. After myelography, CT was performed on a GE 9800 unit with 120 kV and 70 to 140 mAs. Lateral scout images were obtained for planning locations of horizontal sections. Five- to ten-millimeter contiguous sections were then obtained through the region of interest in all three patients and additional direct 3-mm sagittal images were available in one.

Evaluation of each study included level and shape of spinal cord terminus with correlated level of bony agenesis, any bony central spinal canal stenosis, and any intrinsic spinal cord abnormality. Dysraphic anomalies of the vertebral bodies were characterized, and the relative difficulty in assessing osseous defects on MR scans was determined subjectively.

Results

Level of Vertebral Agenesis

In all but one case, the level of vertebral column termination could be determined on either MR images or on plain films (Fig. 1). In that isolated instance, overlying bowel gas prevented the exact identification of the last vertebrae on plain films. In the remaining patients, the last vertebrae was T8–T9 in three patients (25%) (Fig. 2), T10–T12 in no patient (0%), L1–L5 in two patients (17%), and S1 or lower in seven patients (58%) (Tables 1 and 2). Below the last intact vertebrae, the terminal one to two vertebrae were hypoplastic (Figs. 1 and 3–5). All our subjects had symmetrical sacral agenesis; none had hemisacrum. In one patient, the lower sacrum and the coccyx were identified despite absent vertebrae in the lower thoracic, entire lumbar, and upper sacral regions (Fig. 6).

Level and Shape of Cord Terminus

In all patients the cord terminated above the last intact vertebral body. In one patient, lateral views from the myelogram were not available; therefore, the exact location of the cord terminus could not be determined. Both MR and CT-myelography adequately showed the level of the cord terminus, but MR more accurately demonstrated its shape because direct sagittal images can be obtained. However, no direct comparisons were made between the imaging techniques in the same patient.

The caudal end of the spinal cord appeared blunted and angulated with the dorsal aspect extending farther inferiorly than the ventral portion (wedge-shaped) in six of the seven patients evaluated with MR studies (Table 1 and Figs. 2, 3, and 7). In the remaining case, a fibrolipoma of the filum terminale tethered the cord, which, therefore, had a gradually tapered shape (Fig. 4). In one patient, CT-myelography dem-

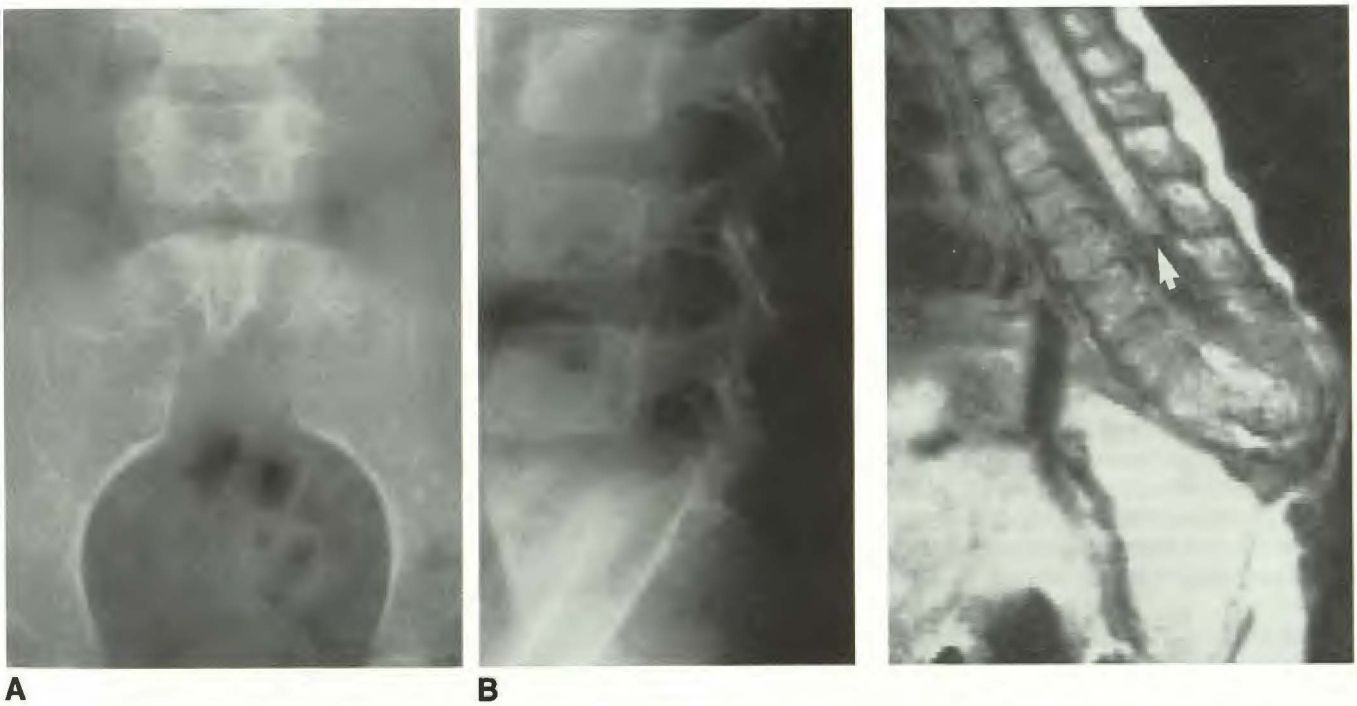

Fig. 1.—Patient 13. 4-year-old girl. Anteroposterior (*A*) and lateral (*B*) radiographs show level of vertebral column termination at S1. Iliac wings articulate with L5 and hypoplastic S1 vertebrae.

Fig. 2.—Patient 5. 8-month-old boy with severe caudal regression. Sagittal spin-echo image, 650/40. Vertebral column terminates at T8 vertebral body (confirmed with radiographs), a level previously considered to be incompatible with survival. The T8 spinous process is absent and the spinal canal is markedly stenotic below the last intact vertebrae, T7. The characteristic wedge-shaped cord terminus (*arrow*) is seen opposite T5 vertebral body.

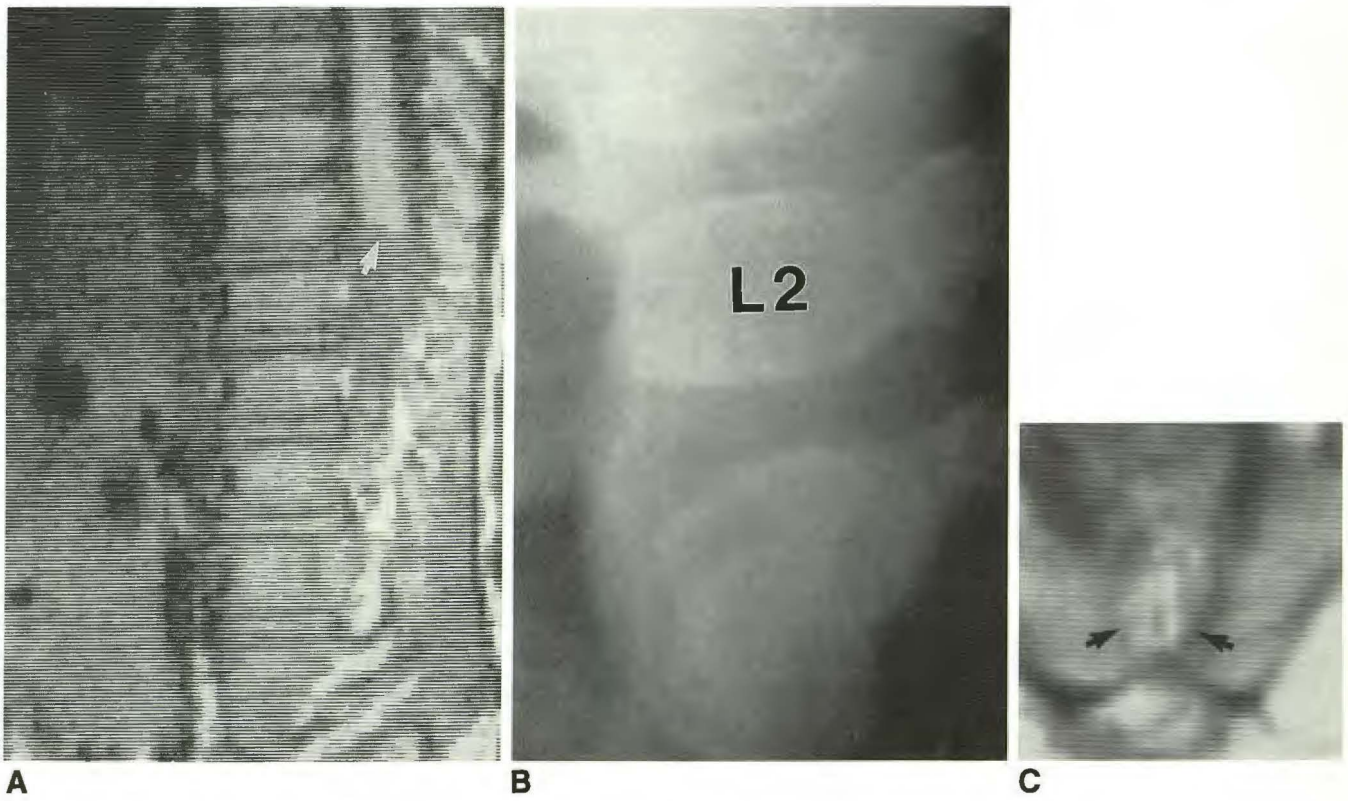

Fig. 3.—Patient 1. 7-year-old boy born to a woman with diabetes mellitus.
***A*, Sagittal spin-echo image, 1000/50, shows caudalmost vertebrae, L4, to be hypoplastic and fused to L3, the last intact vertebral body. Cord ends in characteristic wedge shape (*arrow*) at T10 vertebral body level.**
***B*, Lateral radiograph confirms fusion of hypoplastic L4 vertebral body to L3.**
C, Axial spin-echo image, 1000/40. Narrow bony spinal canal (*arrows*) is entirely filled with fat, and no thecal sac is visualized. Iliac bones articulate with L4 vertebrae.

onstrated the characteristic wedge-shaped cord terminus (Fig. 5). Of the remaining five patients assessed by myelography and CT, the shape of the cord ending appeared slightly bulbous in two and was inadequately visualized in three.

Intraspinal Lesions

MR. One 16-year-old patient had a low-lying cord terminus and a thickened, fatty filum. The cord ended at the level of the L3–L4 interspace (below the lowest accepted level of mid-L2 by age 12 years) [4], and a small central area of prolonged T1 (syringohydromyelic cavity/myelomalacia) was present in the substance of the caudal spinal cord (Fig. 4). This patient had anomalies of the extremities, anal atresia, and congenital hydrocephalus. Spinal stenosis was not present.

Myelography and CT. In a 1-month-old patient, a stretched spinal cord ended in a lipomyelomeningocele at approximately the S3–S4 level. Inadequate visualization of the internal architecture of the cord prevented assessment for cord cavitation or myelomalacia. No spinal stenosis was evident.

Spinal Canal Stenosis

MR. Five of the seven patients had severe central spinal canal bony stenosis extending for several levels below the last intact vertebrae (Figs. 3 and 7). The patient with filum fibrolipoma was one of the two cases without spinal canal stenosis (Fig. 6).

Myelography and CT. Bony spinal stenosis was present at several of the caudalmost vertebral levels in one of the three patients in whom canal size could be evaluated (axial CT and lateral radiographic images were not available through the region of interest in others). The patient with lipomyelomeningocele was one of the two without central spinal stenosis.

Associated Bony Abnormalities

Plain films and CT scans exquisitely identified the dysraphic posterior elements, fusion of vertebral bodies, spina bifida, and a duplex spinous process (Table 2 and Fig. 6D). MR images also demonstrated absent or hypoplastic spinous processes in three patients (Fig. 2), vertebral body fusion in two patients (Fig. 4A), and widened neural foramina in one patient.

Discussion

The caudal regression syndrome occurs in one of 7500 births [1]. Although 16% of patients with caudal regression are offspring of mothers with diabetes mellitus, only 1% of

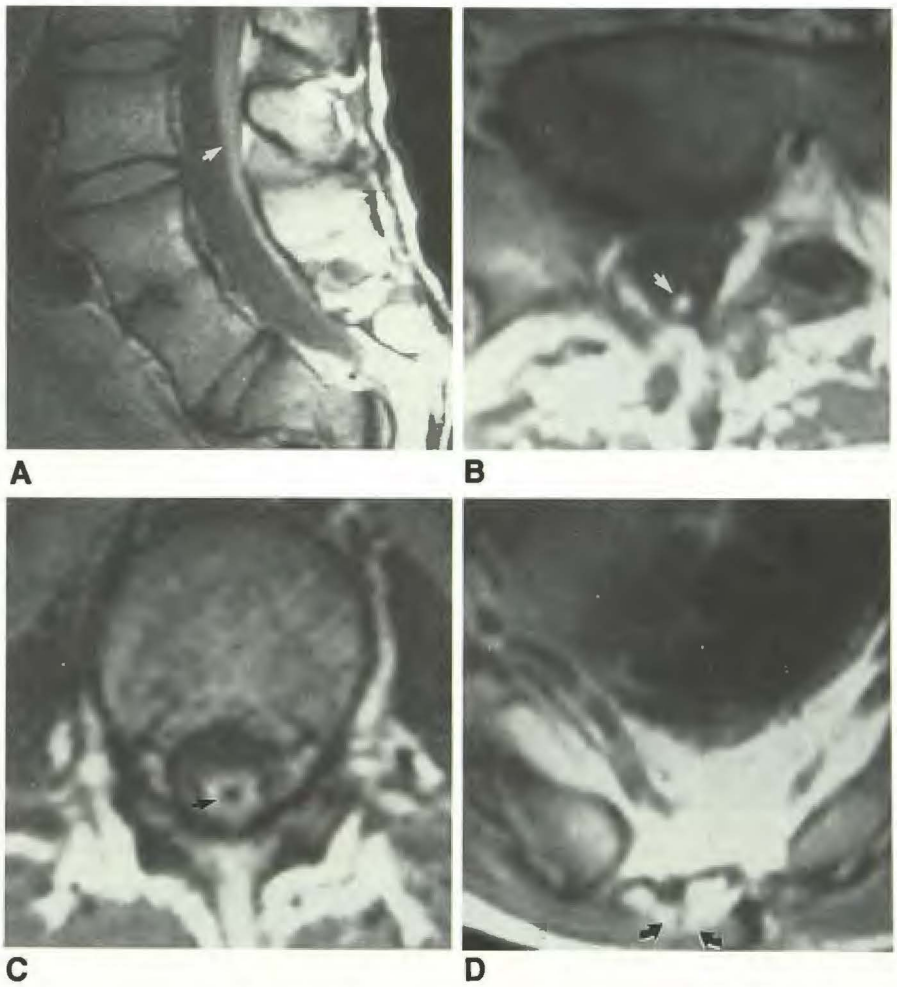

Fig. 4.—Patient 2. 16-year-old boy with caudal regression syndrome also presented with findings suggestive of tethered spinal cord syndrome.

***A*, Sagittal spin-echo image, 702/39. Caudal end of cord is low-lying with tapered and stretched cord terminus (*arrow*) ending opposite L3–L4 interspace. L4 and L5 vertebral bodies are fused, S2 vertebrae is hypoplastic, and vertebrae below S2 level are absent.**

***B*, Axial spin-echo image, 650/35, through L5 level reveals fibrolipoma of filum terminale (*arrow*) to be the cause of tethering.**

***C*, Axial spin-echo image, 650/35, at L2 shows myelomalacia/syringohydromyelia (*arrow*) in caudal end of spinal cord, a finding not uncommon with tethering.**

***D*, Axial spin-echo scan, 650/35, immediately below hypoplastic S2 vertebral body shows a narrow spinal canal (*arrows*) filled with fat and devoid of thecal sac.**

children with diabetic mothers have the caudal regression syndrome [5, 6]. Hereditary factors appear to play no significant role and most of the patients have normal chromosomes [7].

Caudal regression syndrome consists of absence of a portion of the caudal spine, frequently in conjunction with various urologic, neurologic, and orthopedic problems. Our observations confirm that more extensive vertebral regression correlates with more severe associated abnormalities. For example, patients with coccygeal absence alone typically remain asymptomatic, whereas patients with lumbar aplasia develop lower extremity motor and sensory dysfunction as well as urinary incontinence. Moreover, regression above the T10 level has not previously been reported to be compatible with life [8] (Table 1 and Fig. 2).

These patients usually present with orthopedic problems (including hip dislocations and equinovarus deformities of the feet), with urinary symptoms associated with impairment of detrussor function (in those with more than one missing sacral segment), or (in severe cases) with urologic anomalies such as bladder extrophy [9]. Neurologic manifestations include motor and sensory deficits that usually correspond to the level of vertebral agenesis; in some patients, however, sensory function persists below the level of vertebral regression [9]. The sensory examination remains an unreliable index to the function of the urinary bladder, since patients with urinary incontinence may have full perineal sensation [9]. The rectum usually retains normal ganglia and nerve fibers [2, 7]. Neurologic deficits may be static or progressive and, in the latter situation, may be amenable to surgical treatment [2]. Progressive symptoms may result from dural sac stenosis, narrowing of the caudalmost bony spinal canal, compression of the spinal cord by bony excrescences arising from the vertebral bodies, myelomeningocele, lipomyelomeningocele, tight filum syndrome, lipoma, diastematomyelia, and adhesive arachnoid bands. Static neurologic manifestations probably result from spinal cord dysplasia or dysplastic nerve roots; the degree of dysplasia increases in the more caudal segments [1, 2, 10].

In the present study, MR scans depicted the level of vertebral regression in all cases. Although CT more readily characterized osseous vertebral abnormalities, sagittal and axial MR scans clearly depicted central spinal canal stenosis for various lengths above the level of vertebral regression in five of seven patients (two patients had no bony central spinal stenosis). MR also identified a tethered cord with a filum fibrolipoma, which was the cause of progressive neurologic deficits. The literature reports that the thoracolumbar spine is

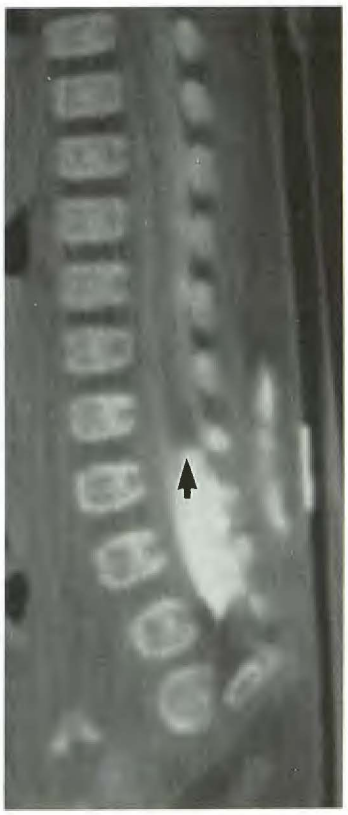

Fig. 5.—Patient 9. 3-week-old with dysplastic kidneys. Direct sagittal CT scan after a myelogram shows abnormal, abruptly terminated, horizontal cord terminus (*arrow*) at T9–T10 interspace. Horizontal termination of cord in this patient differs slightly from characteristic wedge shape seen in other patients. L2, the caudalmost vertebrae, is hypoplastic.

normal above the agenetic segments in only 65% of patients [1], and MR images in our study clearly depicted two cases of congenital vertebral body fusion, one case of hypoplastic spinous process, and two cases of absent spinous processes.

The shape of the cord terminus was well depicted on all MR scans and by myelography and/or CT in three of six patients. In contradistinction to the normal conus medullaris, which smoothly and gradually narrows, the spinal cord ended in a wedge shape (the dorsal aspect of cord extending farther caudally) in seven of eight patients with adequate images and without evidence of a tethering lesion (Figs. 2, 3, and 7). This characteristic wedge-shaped appearance may explain the fact that the sensory deficit may occur at a lower level than the motor deficit in some of these patients. We postulate that the imaging and pathologic findings in the caudal regression syndrome may be explained by the embryological development of the spinal cord and the vertebrae [11] (Figs. 8–10).

The primitive streak and Hensen's node define the caudal end of the embryo and give rise to the mesodermal layer and the midline notochordal process [11, 12] (Fig. 8). The notochord elongates in a cranial direction by addition of cells to its caudal aspect and induces the transformation of the overlying ectoderm into neuroectoderm (neural plate) (Fig. 8). The induction is regional, with the more cranial portion of the notochord influencing the formation of the forebrain and the caudal portion affecting the spine [12]. Since the head and the upper cervical spinal structures are usually normal in patients with caudal regression syndrome, the rostral noto-

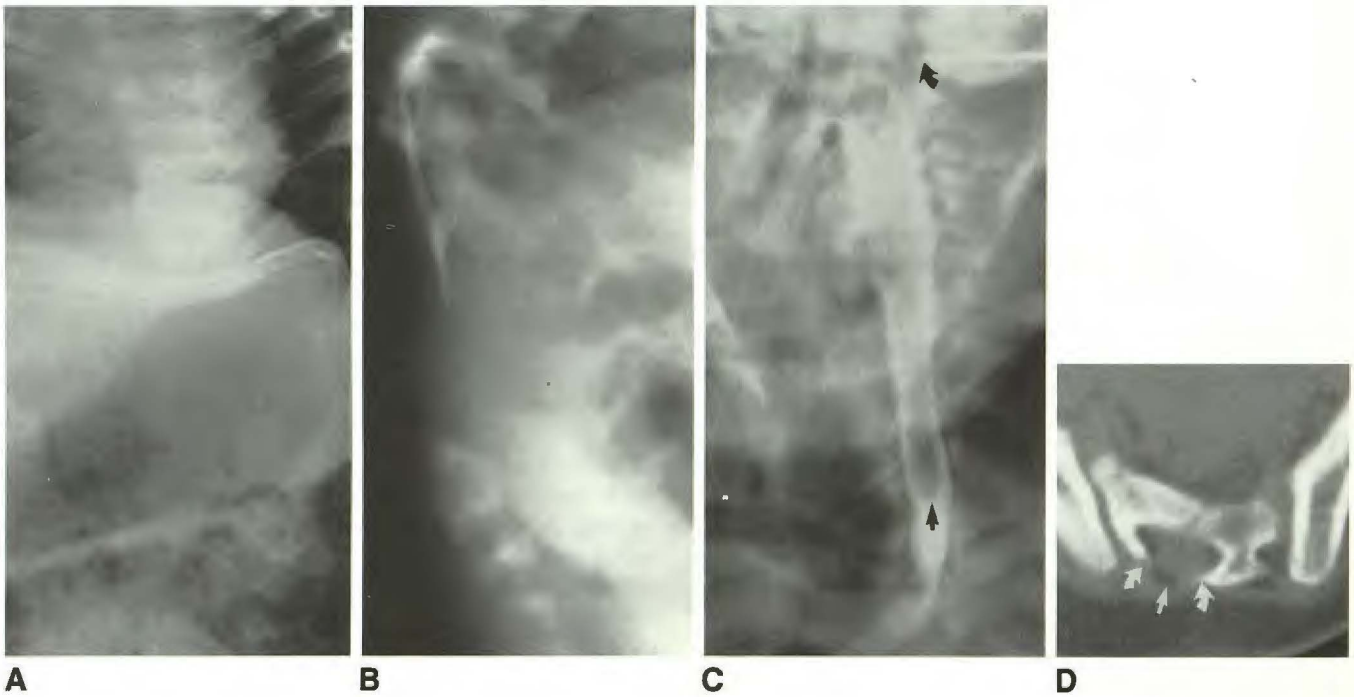

Fig. 6.—Patient 11. 2-year-old girl born with anal atresia.

A and *B*, Anteroposterior (*A*) and lateral (*B*) radiographs reveal absence of vertebrae from T10 to mid-sacrum.

C, Myelogram performed via C1–C2 puncture (*curved arrow* points to myelogram needle at C1–C2) shows cord terminus to be at mid-thoracic level (*straight arrow*). Contrast material did not enter sacral level.

D, Noncontrast axial CT scan shows soft-tissue density material (*straight arrow*) within caudal sacral spinal canal. Spina bifida of sacral vertebrae is evident (*curved arrows*).

chord must have developed and induced the ectoderm in those regions. Hence, degeneration of the notochord and the neural tube in the caudal region as seen in this syndrome must be a later phenomenon.

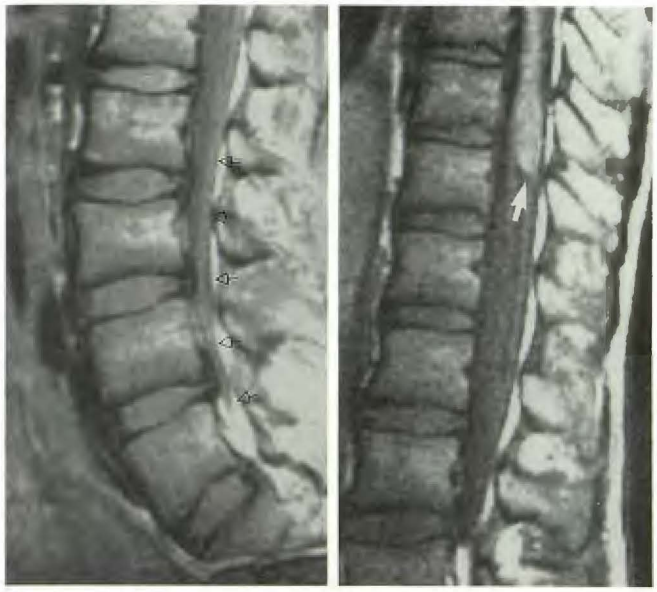

Fig. 7.—Patient 3. 15-year-old boy with neurogenic bladder.
***A*, Sagittal spin-echo images, 1000/20. Last vertebrae is S2 and bony spinal canal is stenotic from L2 inferiorly (*arrows*).**
***B*, Sagittal spin-echo scan, 1000/20, displays characteristic wedge-shaped cord terminus (*arrow*) at mid-T11 vertebral body level.**

The degeneration of the caudal spinal cord with sparing of the rostral cord as well as our finding of the characteristic wedge-shaped spinal cord terminus extending farther caudally along its dorsal, compared with its ventral, aspect may be explained by the peculiar circulation pattern during development. The circulatory system functions by age 21 days [11], and the neural tube is the first part of the embryonic body to receive blood vessels spreading beyond their primary location in the walls of yolk sac and digestive tube [11]. In fact, the blood vessels reach and begin to spread over the ventral surface of the neural plate even before the latter has completely closed to form a tube [11]. Work with the pig embryo reveals that the capillary network, which is initially continuous with that of the adjacent mesenchyme, develops first on the ventrolateral surface of the cord, then on the ventral, and finally on the dorsal surface [13]. Given this vascular distribution, delivery of teratogenic substances would probably affect the notochord and the ventral neural tube to a greater degree than the dorsal neural tube. Moreover, because of the increased metabolic activity in Hensen's node, the circulation and the delivery of circulation-borne teratogen may be increased in this caudal region (Fig. 10). Rumplessness (a condition in fowls that is equivalent to caudal regression) has been induced in chickens with insulin and other sulfur-containing blood-borne molecules, but the exact association between maternal diabetes mellitus and caudal regression syndrome remains unclear [2].

The previous discussion makes it apparent that degeneration of the notochord in the region of Hensen's node may occur without degeneration of the more rostral notochord. Conceivably, a focal delivery of teratogen or a focal infectious

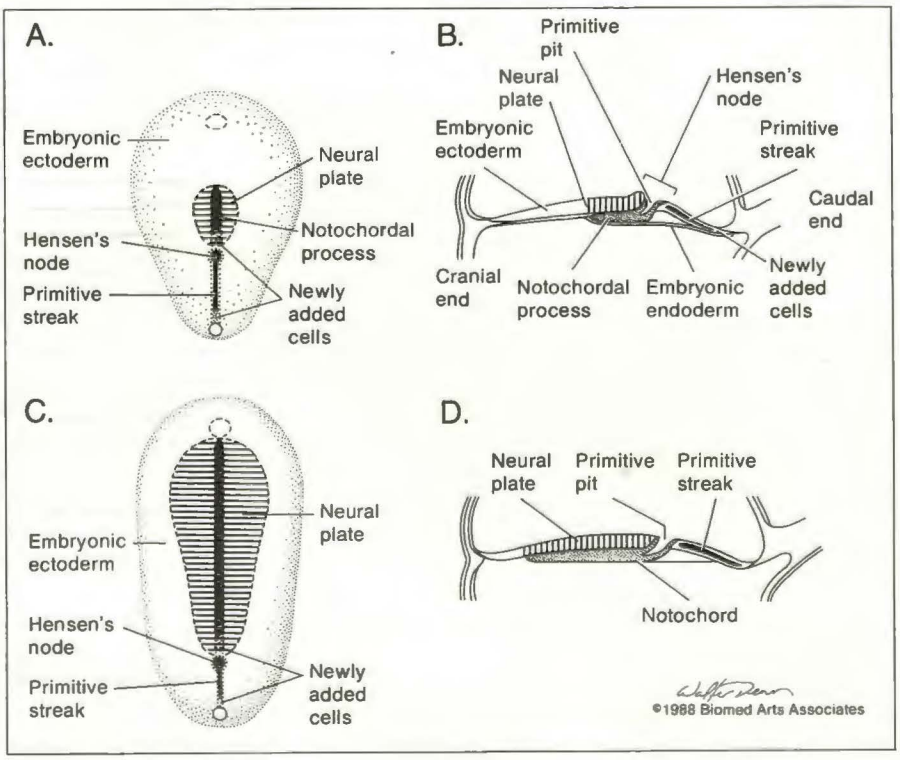

Fig. 8.—Illustration of neural ectoderm induction. Dorsal views (*A* and *C*) of embryonic disk and sagittal sections (*B* and *D*) through embryo show primitive streak and its thickened cranial portion, Hensen's node, giving rise to midline notochord. Notochord induces overlying ectoderm to differentiate into neuroectoderm. Primitive streak eventually degenerates and disappears. Caudal end of neural tissue (above Hensen's node) and notochord blend into an aggregate of cells referred to as caudal cell mass (see Fig. 10). (Modified with permission from Moore [11], pages 52–54.)

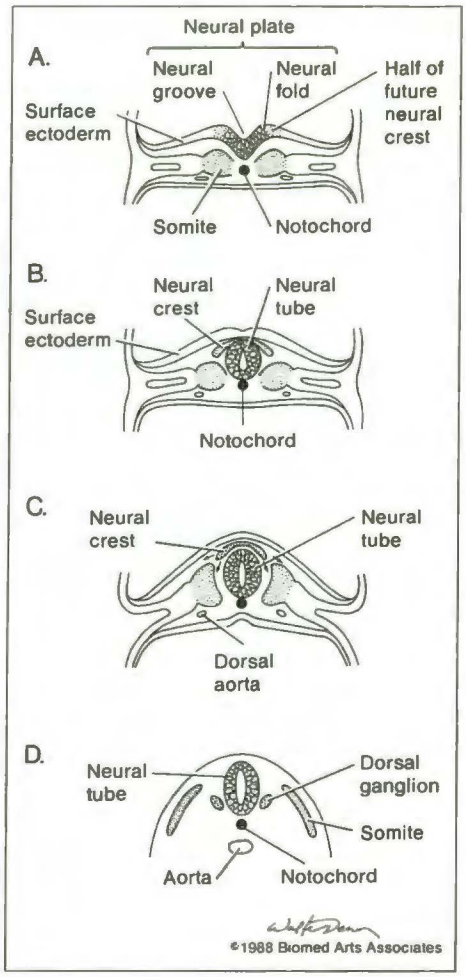

Fig. 9.—Illustration of neurulation and disjunction.

***A*, Transverse view. Neural plate dorsal to notochord invaginates along its central axis to form neural groove and neural folds.**

***B*, Transverse view. Neural folds fuse dorsally in midline to form neural tube (neurulation). During the process of disjunction (of neuroectoderm from cutaneous ectoderm), closure of neural tube squeezes neural crest cells from neuroectoderm/surface ectoderm junction.**

***C*, Transverse view. Neural crest cells then migrate (*arrows*) and eventually give rise to various structures including (*D*) dorsal ganglia. (Modified with permission from Moore [11].)**

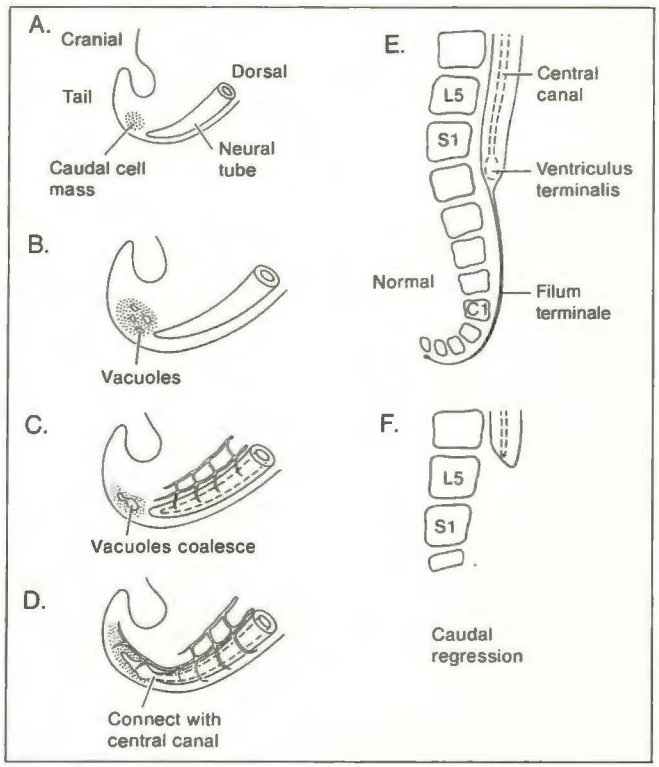

Fig. 10.—Illustration of caudal spinal cord formation. Lateral views (*A–E*) demonstrate vacuoles developing (canalization) in caudal cell mass, which is inferior to portion of neural tube derived from neurulation (Fig. 9). Vacuoles coalesce and make contact with central canal of neural tube. The structures derived from canalization phase then undergo elongation and narrowing (retrogressive differentiation) to form filum terminale, tip of conus, and ventriculus terminalis.

Because, as noted in the text, early blood vessels develop first on ventrolateral surface of cord (*C*, *D*) and blood flow is highest to caudal regions (around Hensen's node), teratogenic substances would be delivered to caudal end of spinal cord and could result in degeneration of caudal end of neural tube and the structures derived from the caudal cell mass (*F*). If a high concentration of teratogens were delivered to the ventral cord (as a result of greater ventral blood supply), the characteristic wedge-shaped cord terminus (longer dorsally) would result. (Modified with permission from Lemire et al. [19], pages 73 and 78.)

or ischemic process could spare the caudalmost notochord and caudal cell mass and result in formation of thoracic and lower sacrococcygeal vertebrae with absence of lumbar vertebrae, as seen in one of our patients (Fig. 6).

Even though the dorsal aspect of the spinal cord extends farther inferiorly than the ventral aspect, the level of bony agenesis corresponds to the level of the last ventral root. This is explained by our postulate of a focal insult to the notochord and the ventral cord, because the notochord influences the formation of the vertebral body and the ventral region of the spinal cord appears to be the key inducer of the neural arches of the vertebral column [14].

Dorsal root ganglia development at several levels caudal to the last vertebrae and the corresponding last ventral nerve root has been described [9]. This phenomenon can also be explained by analysis of the embryological development of the spine (Fig. 9). At the time of disjunction, closure of the neural plate squeezes the neural crest cells from the ectoderm. The extruded crest cells briefly form a loosely aggregated midline mass dorsal to the spinal cord and subsequently migrate to form dorsal root ganglia, autonomic ganglia adjacent to the dorsal aorta, cells of the adrenal medulla, and melanocytes [12, 15, 16] (Fig. 9). Removal of the notochord and neural tube after the crest cells have reached their destination does not affect the survival or differentiation of cells forming the enteric nervous system and autonomic ganglia [17]; the presence of ganglionic cells in the intestine of patients with caudal regression syndrome suggests that the teratogenic insult occurs after the migration of the neural crest cell anlage of these structures. A restricted period of development occurs, however, during which the neural crest cells that compose the dorsal ganglia will perish shortly after

migration if the neural tube is removed. After establishing connections with peripheral targets, these cells increasingly depend on trophic support from target organs rather than CNS influence for further survival [18]. If the teratogenic insult occurs after the critical stage of neural tube dependence, some neural crest cells may survive and develop into dorsal root ganglia at several levels caudal to the last vertebral body and ventral root. The longer dorsal spinal cord may then provide the substrate for central connections needed by these dorsal ganglia. Alternatively, after an earlier exposure to teratogens, the persistent dorsal cord could maintain CNS influence, enabling the dorsal ganglia to survive the critical stage and subsequently establish connections with peripheral targets. We find no evidence to support one theory over the other and it may be that both are valid.

In a majority of patients with caudal regression syndrome, neural crest cells forming the dorsal root ganglia perish, presumably as a result of neural tube degeneration during the critical period after migration. This degeneration predictably results in absence of spinal ganglia below the level of the lowermost vertebrae, as seen in most patients with caudal regression. As a result of absence of both notochord and neural tube, the meninges, vertebrae, and paraspinous musculature fail to develop. Urinary abnormalities, seen in the majority of patients, probably result from disruption of sensory input and motor output. Lesser abnormalities of the notochord and neural tube would be expected to occur immediately cranial to the level of complete degeneration; indeed, stenosis of the dural sac and malformations of vertebrae such as narrow bony canal and vertebral dysraphism are seen in many patients, and in some instances are responsible for spinal cord tethering. Other causes of tethering result from disruption of neurulation, disjunction, canalization, or retrogressive differentiation (Figs. 9 and 10), all of which are more likely to occur when the initial processes of cord development are disturbed [19].

In conclusion, we have described MR findings in seven patients with caudal regression syndrome. MR effectively depicted the level of vertebral regression and the presence of central spinal canal stenosis as well as the vertebral dysraphic anomalies in our patients. MR was subjectively superior to plain films and CT-myelography at demonstrating the shape of the caudal end of the spinal cord and the cause of cord tethering (no direct comparisons were made between the techniques in the same patient). The cord often ended in a characteristic wedge-shaped terminus (longer dorsally), which may be a specific finding in caudal regression syndrome. We have described an unusual finding of preservation of the lower sacrum and coccyx with regression of the lumbar spine in a patient, and, for the first time, surviving individuals with vertebral regression above the T10 level. We propose a theory based on embryological development to explain the various clinical, pathologic, and radiographic findings in the caudal regression syndrome.

REFERENCES

1. Nadich TP, McLone DG, Harwood-Nash DC. Spinal dysraphism. In: Newton TH, Potts DG, eds. *Computed tomography of the spine and spinal cord,* vol. 1. San Anselmo, CA: Clavadel Press, **1983**:299–354
2. Pang D, Hoffman JH. Sacral agenesis with progressive neurological deficit. *Neurosurgery* **1980**;7:118–126
3. Raghavan N, Barkovich AJ, Edwards M, Norman D. MR imaging in the tethered spinal cord syndrome. *AJNR* **1989**;10:27–36
4. Fitz CR, Harwood-Nash DC. The tethered conus. *AJR* **1970**;125:515–523
5. Passarge E, Lenz W. Syndrome of caudal regression in infants of diabetic mothers: observations of further cases. *Pediatrics* **1966**;37:672–675
6. Dunn V, Nixon GW, Jaffe RB, Condon VR. Infants of diabetic mothers: radiographic manifestations. *AJR* **1981**;137:123–128
7. Sarnat HB, Case ME, Grauiss R. Sacral agenesis. *Neurology* **1976**;26:1124–1129
8. Banta JV, Nichols O. Sacral agenesis. *J Bone Joint Surg [Am]* **1969**;4:693–703
9. Smith ED. Congenital sacral anomalies in children. *Aust NZ J Surg* **1959**;29:165–176
10. Brooks BS, El Gammal T, Hartlage P, Beveridge W. *AJNR* **1981**;2:319–323
11. Moore KL. *The developing human*, 4th ed. Philadelphia: Saunders, **1988**:52–54, 365–367
12. Karp G, Berrill NJ. *Development: neurulation and primary induction*, 2nd ed. San Francisco: McGraw-Hill, **1981**:361–396
13. Hoskins ER. On the vascularization of the spinal cord of the pig. *Anat Rec* **1914**;8:371–390
14. Kallen B. Early embryogenesis of the central nervous system with special reference to closure defects. *Dev Med Child Neurol [Suppl]* **1968**;16:44–53
15. Kirby ML, Bockman DE. Neural crest and normal development: a new perspective. *Anat Rec* **1984**;209:1–6
16. Newgreen DF, Erickson CA. The migration of neural crest cells. *Int Rev Cytol* **1986**;103:89–145
17. Teillet M, Le Douarin NM. Consequences of neural tube and notochord excision on the development of the peripheral nervous system in the chick embryo. *Dev Biol* **1983**;98:192–211
18. Kalcheimm C, Le Douarin NM. Requirement of a neural tube signal for the differentiation of neural crest cells into dorsal root ganglia. *Dev Biol* **1986**;116:451–466
19. Lemire RJ, Loeser JD, Leech RW, Alvord EC. *Normal and abnormal development of the human nervous system.* Hagerstown, MD: Harper & Row, **1975**:54–83